

Nonlinear Analysis of Pin-Jointed Assemblies with Buckling and Unilateral Members

K.Yu. Volokh¹

Abstract: A computational framework is described for modeling pin-jointed structures comprising unilateral cable members and slender struts. The deep postbuckling behavior of struts is considered by means of ‘elastica’ analytical approximation. Prestressing is allowed. The proposed approach is incorporated into equilibrium path following procedures and illustrated in numerical examples.

keyword: nonlinear analysis, buckling, bifurcation, cable

1 Introduction

Pin-jointed assemblies with buckling and unilateral members are used for modeling various structural frameworks at different length scales: cable nets, tensegrity systems, space trusses at the macroscale; cytoskeletal structures at the mesoscale [Ingber (1993,1998)]. Traditionally, analysis of pin-jointed assemblies is based on the assumption that all structural members are ideal struts resisting tension and compression linearly in accordance with Hooke’s law. Such framework is used for both linear and nonlinear analyses, where strains are small and displacements may be large as, for example, in case of cable nets [Krishna (1978); Buchholt (1985); Szabo and Kollar (1984); Volokh (1999)]. This approach, however, is unable to treat possible local buckling of individual compressed members or ‘switching off’ of cable members. Mentioned ‘irregularities’ of structural behavior are of interest for space structures [Kondo and Atluri (1985); Tanaka et al. (1985)] and cytoskeletons of living cells [Coughlin and Stamenovich (1997); Volokh et al. (2000)].

In principle the local buckling of compressed members may be treated by considering these members partitioned into beam elements. This approach is time consuming and computationally disadvantageous because of ill con-

ditioning induced by the sub-partitioning and necessity of additional branching during the equilibrium path following. Kondoh and Atluri (1985) proposed to directly consider the postbuckling of struts by using the ‘elastica’ solution. They used power series to approximate elliptic integrals involved in this solution. These authors explicitly derived tangent stiffness and accounted for the postbuckling of 10-15% chord shortening. Volokh et al. (2000) used a different strategy for the local postbuckling. They fitted the implicit ‘elastica’ solution by polynomials and used the obtained analytical expressions in the subsequent numerical analysis. Within this framework the 100% chord shortening, or the postbuckling bending into a ring, is available. The main drawback, however, was the necessity to fit every strut member by polynomials independently. No general polynomial approximation was derived.

An explicit and universal, independent of material and geometrical properties of individual struts, polynomial solution of the ‘elastica’ problem is given in this note. This solution allows for 100% chord shortening in the postbuckling range of compressed members. This solution together with the proposed treatment of unilateral response of cables and possible initial prestressing is used for computational formulation and nonlinear numerical analysis of pin-jointed assemblies with buckling and unilateral members.

2 Formulation

2.1 Kinematics

Axial force p and chord elongation Δ are main conjugate variables. It is important to realize *that the chord elongation is not necessarily the real member elongation*. The chord elongation takes the form:

$$\Delta = l - L \quad (1)$$

¹ Technion-I.I.T. Haifa Israel (e-mail: cvolokh@aluf.technion.ac.il)

$$l = \sqrt{(X_j + u_j - X_s - u_s)^2 + (X_{j+1} + u_{j+1} - X_{s+1} - u_{s+1})^2 + (X_{j+2} + u_{j+2} - X_{s+2} - u_{s+2})^2} \quad (2)$$

$$L = \sqrt{(X_j - X_s)^2 + (X_{j+1} - X_{s+1})^2 + (X_{j+2} - X_{s+2})^2} \quad (3)$$

where L and l are the initial (reference) and final (current) chord lengths of a member respectively; u and X are nodal displacements and coordinates respectively.

To consider a two-dimensional problem it is necessary to drop the last term under the roots in Eqs.2 and 3. To this end, there is no essential difference between 2D and 3D problems in principle. This is in contrast to frameworks with rigid joints where the 3D problem is significantly more complicated because of kinematics.

2.2 Constitutive relation for struts

In order to derive the desirable relation for the buckling strut it is necessary first to express explicitly the ‘elastica’ solution for a hinged strut. The solution of the postbuckling or ‘elastica’ problem for a clamped-free column (Fig1.a) may be written as follows [Timoshenko and Gere (1961)]:

$$\frac{L}{2} = \sqrt{\frac{EI}{p}} K \left(\sin^2 \frac{\alpha}{2} \right) \quad (4)$$

$$\frac{l}{2} = 2 \sqrt{\frac{EI}{p}} E \left(\sin^2 \frac{\alpha}{2} \right) - \frac{L}{2} \quad (5)$$

$$K(m) = \int_0^{\pi/2} \frac{d\varphi}{\sqrt{1 - m \sin^2 \varphi}}; E(m) = \int_0^{\pi/2} \sqrt{1 - m \sin^2 \varphi} d\varphi$$

where α is the edge slope; $L/2$ is the initial length of the straight column and $l/2$ is its ‘vertical length’ after buckling; K and E are complete elliptic integrals of the first and second kind correspondingly; EI is a bending stiffness. This result may also be interpreted as the solution of the buckling problem of the hinged column shown in

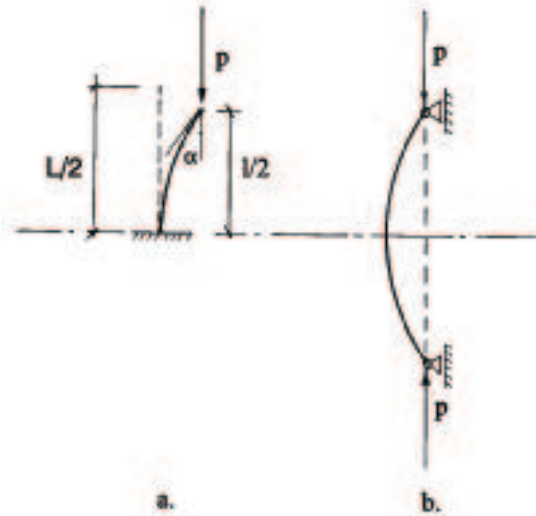


Figure 1 : ‘Elastica’ problem (a) and its extension to the hinged strut (b).

Fig1.b. In the latter case l is the column chord length after buckling.

In order to establish the postbuckling relation between the axial force p and chord elongation $\Delta = l - L$ it is necessary to exclude the edge slope α from Eqs.4 and 5. Unfortunately, an exact analytical solution of this problem is not available. An approximate polynomial solution, however, may be obtained. In order to find this solution, Eq.4 is rewritten in the following form:

$$p^* \equiv \frac{p}{p_{cr}} + 1 = -\frac{4}{\pi^2} K^2 + 1 \quad (6)$$

where p^* is a ‘relative’ axial force; $p_{cr} = \pi^2 EI/L^2$ is an absolute magnitude of the critical buckling load for the hinged column. It was taken into account that compression is negative in sign. The relative force is zero where the axial load is the buckling load: $p = -\pi^2 EI/L^2$. Excluding the

axial force from Eq.5 with the help of Eq.4 and introducing the chord elongation, Eq.5 takes the following form:

$$\varepsilon \equiv \frac{\Delta}{L} = 2 \left(\frac{E}{K} - 1 \right) \quad (7)$$

It is remarkable that right hand sides of Eqs.6 and 7 are not problem specific, that is they do not depend on ge-

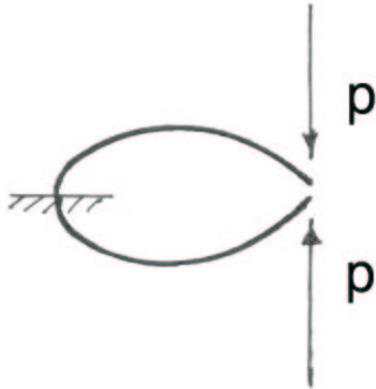


Figure 2 : Postbuckling bending into a ring.

ometrical and physical properties of the considered column. The latter prompts an idea to relate p^* and ϵ by tabulating the right hand sides of Eqs.6 and 7 for arguments of elliptic integrals pointwisely and then to fit the tabulated relation by polynomials. In order to accomplish this plan, it is necessary first to determine the range of the elliptic integrals argument where the tabulation will take place. It is evident that the postbuckling begins with $\alpha = m = 0$. To obtain the second limit of the argument range, we restrict our consideration to the column buckling into a ring as shown in Fig.2. In this case the following equation is solved:

$$\frac{l}{L} = 2 \frac{E(m)}{K(m)} - 1 = 0.$$

Its appropriate solution is $m = 0.826 \rightarrow \alpha = 130.69^\circ$. The tabulated relation $p^* \sim \epsilon$ for $m \in [0, 0.826]$ is shown in Fig.3. The bold line depicts 1001 points where the tabulation has been carried out. To produce the polynomial fit, the command 'Fit' of Mathematica [Wolfram (1999)] was used. The standard least squares fit underlies this Mathematica procedure. Various polynomial expressions are available and even low order polynomials provide very good fit to the tabulated data (Fig.3). These polynomials take the form:

$$p^* = \begin{cases} 0.302976\epsilon - 0.80794\epsilon^2 \\ 0.580876\epsilon + 0.146604\epsilon^2 + 0.731706\epsilon^3 \\ 0.470935\epsilon - 0.530524\epsilon^2 - 0.477617\epsilon^3 - 0.65546\epsilon^4 \end{cases} \quad (8)$$

Though the second order polynomial is very close to exact data and the third order polynomial visually coincides with the exact data the choice of the fourth order polynomial is most accurate, the reason for that is left to the first numerical example (Section 4).

Now $p \sim \Delta$ relation may be written as follows (Fig.4):

$$p = \beta \frac{EA}{L} \Delta + (1 - \beta) \frac{\pi^2 EI}{L^2} \begin{cases} -1 + 0.470935 \left(\frac{\Delta + \Delta_{cr}}{L} \right) \\ -0.530524 \left(\frac{\Delta + \Delta_{cr}}{L} \right)^2 - \\ -0.477617 \left(\frac{\Delta + \Delta_{cr}}{L} \right)^3 \\ -0.65546 \left(\frac{\Delta + \Delta_{cr}}{L} \right)^4 \end{cases} \quad (9)$$

$$\beta = \begin{cases} 1, & \text{if } \Delta \geq -\Delta_{cr}; \Delta_{cr} = \frac{\pi^2 EI}{EAL} \\ 0, & \text{if } \Delta < -\Delta_{cr} \end{cases} \quad (10)$$

2.3 Constitutive relation for cables

The following relation represents a cable member (Fig.5):

$$p = \beta \frac{EA}{L} \Delta \quad (11)$$

$$\beta = \begin{cases} 1, & \text{if } \Delta \geq 0 \\ 0, & \text{if } \Delta < 0 \end{cases} \quad (12)$$

Thus cables are 'switched off' under compression.

2.4 Pre-stressing

Some pin-jointed assemblies, such as tensegrity systems or cable nets, are initially pre-stressed. In this case it is suitable to distinguish between the reference configuration and the member configuration at rest. The latter is

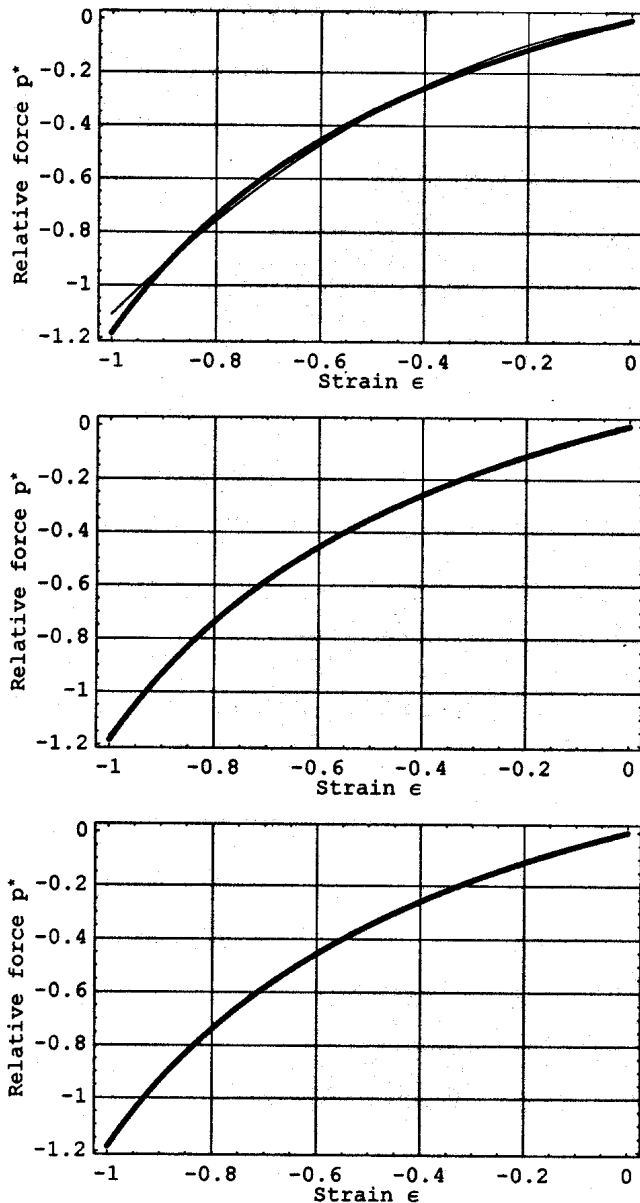


Figure 3 : Second, third, and fourth order polynomial fits. Bold line is the exact data. Third and fourth order polynomials visually coincide with the exact data.

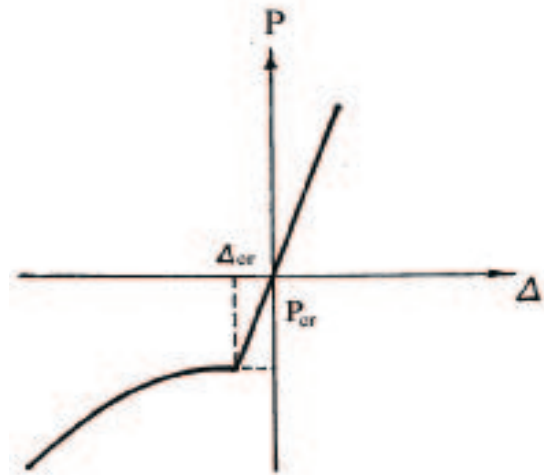


Figure 4 : Constitutive law for struts.

the ‘natural’ configuration where no elongations correspond to zero axial forces. The constitutive relations of Sections 2.2 and 2.3 were defined in such natural configuration. Let a member length be designated \bar{L} in the natural configuration and L in the reference configuration. Then the initial elongation is: $\Delta_0 = L - \bar{L}$. The full elongation is: $\bar{\Delta} = l - \bar{L} = l - L + \Delta_0 = \Delta + \Delta_0$. Thus it is necessary to replace member elongations and lengths in Eqs.9-12 with account of the difference between the natural and reference configurations:

$$\Delta \rightarrow \bar{\Delta} = \Delta + \Delta_0; \quad L \rightarrow \bar{L} = L - \Delta_0 \tag{13}$$

The initial elongation Δ_0 shifts constitutive relations along Δ -axis. This elongation is easily obtained when the member length at rest is known. The reference length can not be arbitrary; it should provide equilibrium of the axial forces produced by the initial elongations at the reference state. The reference length or the initial elongation may be found in the reverse order where the admissible initial axial force p_0 is given. In order to find the initial elongation Δ_0 corresponding to the given p_0 it is necessary to substitute from Eq.13 into Eq.9 or Eq.11 and then to set: $p = p_0; \Delta = 0, \bar{\Delta} = \Delta_0; \bar{L} = L - \Delta_0$. It is assumed that the elongation with respect to the reference configuration is zero. The thus obtained equation is to be solved for Δ_0 . In the case of linear elasticity, for example, we obtain:

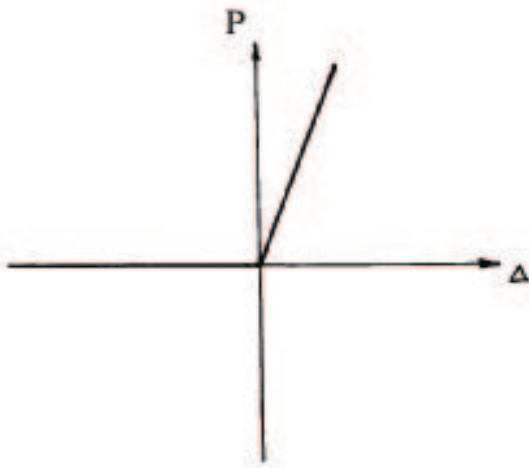


Figure 5 : Constitutive law for cables.

$$\Delta_0 = \frac{p_0 \bar{L}}{EA} = \frac{p_0 L}{EA + p_0}.$$

2.5 Governing equations

In order to formulate governing equations column matrices of member forces \mathbf{p} , elongations Δ and switch functions β are introduced as well as column matrices of nodal displacements \mathbf{u} and 'dead' external nodal forces \mathbf{q} :

$$\mathbf{p} = \{p_1, \dots, p_n\}^T; \Delta = \{\Delta_1, \dots, \Delta_n\}^T; \beta = \{\beta_1, \dots, \beta_n\}^T$$

$$\mathbf{u} = \{u_1, \dots, u_m\}^T; \mathbf{q} = \{q_1, \dots, q_m\}^T$$

where n is a number of structural members and m is a number of nodal degrees of freedom. Kinematic and constitutive relations take the form:

$$\Delta = \Delta(\mathbf{u}) \tag{14}$$

$$\mathbf{p} = \mathbf{p}(\Delta, \beta) \tag{15}$$

Equilibrium equations consistent with the adopted kinematics may be derived from the principle of virtual displacements:

$$\mathbf{q}^T \delta \mathbf{u} = \mathbf{p}^T \delta \Delta \tag{16}$$

Using kinematic equation 14 we obtain:

$$\delta \Delta = \mathbf{B} \delta \mathbf{u} \tag{17}$$

where

$$\mathbf{B} = \frac{\partial \Delta}{\partial \mathbf{u}}; \quad B_{ij} = \frac{\partial \Delta_i}{\partial u_j} \tag{18}$$

is an n by m kinematic matrix.

Substituting Eq.17 into Eq.16 and dropping virtual displacements we obtain equilibrium equations:

$$\mathbf{B}^T \mathbf{p} = \mathbf{q} \tag{19}$$

Eqs.14, 15 and 19 form a closed system of governing equations. To solve these equations numerically the tangent stiffness is usually desirable:

$$\mathbf{K} = \frac{\partial (\mathbf{B}^T \mathbf{p})}{\partial \mathbf{u}} = \mathbf{B}^T \mathbf{C} \mathbf{B} + \mathbf{D} \tag{20}$$

where

$$\mathbf{C} = \frac{\partial \mathbf{p}}{\partial \Delta}; \quad \mathbf{D} = \left. \frac{\partial (\mathbf{B}^T \mathbf{p})}{\partial \mathbf{u}} \right|_{\mathbf{p}=\text{const}} \tag{21}$$

Here \mathbf{C} is the tangent constitutive modular matrix; \mathbf{D} is called geometric stiffness matrix.

An alternative way to derive basic relations is to introduce the strain energy:

$$\Psi = \sum_{i=1}^n \int p_i(\Delta) d\Delta_i \tag{22}$$

We obtain in this case:

$$\mathbf{p} = \frac{\partial \Psi}{\partial \Delta}; \quad (\mathbf{B}^T \mathbf{p}) = \frac{\partial \Psi}{\partial \mathbf{u}}; \quad \mathbf{K} = \frac{\partial^2 \Psi}{\partial \mathbf{u} \partial \mathbf{u}} \tag{23}$$

3 Equilibrium path following

3.1 Basic procedures

To follow the equilibrium path of the given structure in its state space it is useful to introduce a column matrix of the unbalanced nodal forces:

$$\mathbf{g} = \mathbf{B}^T \mathbf{p} - \lambda \mathbf{q} = \mathbf{0} \quad (24)$$

$$\mathbf{K} = \frac{\partial \mathbf{g}}{\partial \mathbf{u}}; \quad \mathbf{q} = -\frac{\partial \mathbf{g}}{\partial \lambda} \quad (25)$$

It is assumed that the external load is initially fixed (\mathbf{q}) and then changes proportionally to parameter λ . A variety of approaches exist for solving Eq.24 with account of Eqs.14 and 15: Crisfield (1991, 1997); Fujii and Okazawa (1997); Keller (1992); Kouhia and Mikkola (1989); Magnusson and Svensson (1998); Riks (1998); Seydel (1994); Sophianopoulos and Michaltsos (2001); Wriggers (1995).

The basic procedure for tracing a monotonically changing equilibrium path is Newton-Raphson algorithm:

Box 1

1. Input: a point on the equilibrium path (\mathbf{u} , λ , \mathbf{g} , \mathbf{K}).
2. Load increment: $\lambda \leftarrow \lambda + d\lambda$ and updating \mathbf{g} .
3. Computation: $d\mathbf{u} = -\mathbf{K}^{-1}\mathbf{g}$.
4. Updating: $\mathbf{u} \leftarrow \mathbf{u} + d\mathbf{u}$ and \mathbf{g} , \mathbf{K} .
5. Go to step 2 if the convergence criterion is satisfied or return to step 3 otherwise.

his algorithm is unable to treat turning points where the equilibrium path does not exist for growing parameter λ . Arc-length continuation is well suited in the latter case:

Box 2

1. Input: a point on the equilibrium path (\mathbf{u} , λ , \mathbf{g} , \mathbf{K}).
2. Arc-length increment: ds .
3. Predictor (initial guess): $\mathbf{y} = \mathbf{K}^{-1}\mathbf{q}$; $d\lambda = ds/\sqrt{\mathbf{y}^T \mathbf{y} + 1}$; $d\mathbf{u} = d\lambda \mathbf{y}$.
4. Updating: $\mathbf{u} \leftarrow \mathbf{u} + d\mathbf{u}$; $\lambda \leftarrow \lambda + d\lambda$; \mathbf{g} , \mathbf{K} .
5. Corrector: $\delta \mathbf{v} = \mathbf{K}^{-1}\mathbf{q}$; $\delta \mathbf{w} = -\mathbf{K}^{-1}\mathbf{g}$; $\delta \lambda = -(\mathbf{d}\mathbf{u}^T \delta \mathbf{w}) / (\mathbf{d}\mathbf{u}^T \delta \mathbf{v})$; $\delta \mathbf{u} = \delta \mathbf{w} + \delta \lambda \delta \mathbf{v}$.
6. Updating: $d\mathbf{u} \leftarrow d\mathbf{u} + \delta \mathbf{u}$; $\mathbf{u} \leftarrow \mathbf{u} + d\mathbf{u}$; $d\lambda \leftarrow d\lambda + \delta \lambda$; $\lambda \leftarrow \lambda + d\lambda$; \mathbf{g} , \mathbf{K} .
7. Go to step 2 if the convergence criterion is satisfied or return to step 5 otherwise.

It may be seen from Box 2, that arc-length parameter ds controls the advance along the equilibrium path and any turning point is readily treated. In contrast to Newton-Raphson procedure (Box 1) the first and subsequent iterations are distinguished and called predictor and corrector steps accordingly. A wide variety of predictors and correctors have been proposed in the literature. It is possible, for example, to find the corrector by applying Newton-Raphson procedure to some augmented system of nonlinear equations, which include Eq.24 together with some arc-length constraint. Such an approach is called 'consistent' by some authors. In this sense, the algorithm given in Box 2 is 'inconsistent'. However, we found it to be very efficient in computations. The latter is the most important criterion for the practical numerical analysis.

The arc-length continuation algorithm should be slightly modified to allow for branch switching. Particularly, the predictor guess \mathbf{y} should be close to the branch emanating from the bifurcation point while $d\lambda$ may be set zero. There are two main strategies to define \mathbf{y} . The first one is to pinpoint the equilibrium point and to find \mathbf{y} as the singular vector of \mathbf{K} at this point. The main drawback of this strategy is the necessity to deal with ill conditioning of matrix \mathbf{K} as the bifurcation point is approached. The second strategy is to define \mathbf{y} as the eigenvector corresponding to the smallest eigenvalue of \mathbf{K} without pinpointing the bifurcation point. In any case the scaling parameter for obtained \mathbf{y} should be fitted by trials-errors. Finally, the stability of the considered path is defined by

positive definiteness of the tangent stiffness matrix \mathbf{K} .

3.2 Modifications

The key feature of the proposed formulation for buckling struts and unilateral cables is discontinuity of tangents to the nonlinear map defined by governing equations. Indeed, partial derivatives $\partial g_i / \partial u_j$ suffer jumps along the equilibrium path because of the accepted constitutive equations 9-12. To treat these jumps numerically the following strategy may be used:

Box 3

1. Input: a point on the equilibrium path (\mathbf{u} , λ , \mathbf{g} , β , \mathbf{K}).
2. Advance by $d\lambda$ or ds along the equilibrium path: steps 2-5 (Box 1) or 2-7 (Box 2).
3. Compute: β_{new} in accordance with Eqs.10 and 12.
4. If $\beta_{new} = \beta$, then: return to 2; else: continue.
5. Switch: $\beta = \beta_{new}$.
6. Advance $d\lambda$ or ds along the equilibrium path: steps 2-5 (Box 1) or 2-7 (Box 2).
7. Compute: β_{new} in accordance with Eqs.10 and 12.
8. If $\beta = \beta_{new}$, then: return to 2; else: continue.
9. Reverse the direction: $d\lambda \rightarrow -2d\lambda$ or $ds \rightarrow -2ds$ and advance along the path.

Here β is a vector of control and it does not change during an incremental step. In other words, the idea is to properly switch constitutive equations, if necessary, after every incremental advance along the equilibrium path. It may happen, however, that after switching the increment leads to the values of β that are different from the initial ones. This means that the solution is on the ‘forbidden’ branches of constitutive curves, for example: $\beta_i = 1$, while $\Delta_i < -\Delta_{cr}$. In this case, it is necessary to return on the ‘admissible’ branch by reversing the direction of the advance without switching β again.

Actually, every switching of β is an implicit branch switching. However, in contrast to the explicit branch-

ing, the emanating path is defined analytically and it is easily accessible! The ‘corner’ points where $\Delta_i = -\Delta_{cr}$ for struts and $\Delta_i = 0$ for cables may be called hidden bifurcation points.

4 Numerical examples

Table 1 : Elastica’s shortening

$\backslash P(\text{kg})$ (cm) $\Delta \backslash$	56.34	59.01	63.955	71.78	84.27	104.59
Exact	0.60	2.38	5.18	8.80	13.02	17.54
‘2’	0.88	2.98	5.70	8.87	12.7	17.51
‘3’	0.52	2.20	5.14	8.88	13.02	17.48
‘4’	0.61	2.39	5.18	8.78	13.03	17.52

4.1 Elastica

The hinged strut shown in Fig.1b is examined with different polynomial approximations of the postbuckling range (Eq.8). The following geometrical and elastic parameters were used for the equilibrium path tracing: $L = 20\text{ cm}$; $A = 1 \times 0.3\text{ cm}^2$; $E = 10^6\text{ kg/cm}^2$. The strut shortenings obtained by using the described numerical procedures are shown in rows 3-5 of Tab.1 for the second, third, and fourth order polynomials correspondingly. The exact solution extracted from Timoshenko and Gere (1961) is given in row 2. The fourth order polynomial better fits the initial postbuckling range.

4.2 Two-member truss

Britvec (1973) examples of the two-member truss are considered: Figs.6-8. All members possess the same characteristics: $L=15\text{ in}$; $A = 1 \times 1/16\text{ in}^2$; $P_{cr} = 29\text{ lb}$. In the first and second loading cases, shown in Figs.6 and 7, the same truss is loaded vertically and its equilibrium path is traced till the point where the full snap-through occurs. The buckling of the left strut only is considered in Fig.6, while the buckling of both struts is considered in Fig.7. Slightly different truss is considered in the third loading case (Fig.8): both struts are allowed for buckling, though only one really buckles, and equilibrium path is traced till the point where the upper strut becomes vertical.

The initial postbuckling behavior in all considered cases is in accordance with the analytical predictions of Britvec (1973). There are interesting features of the deep postbuckling behavior, which cannot be predicted analyti-

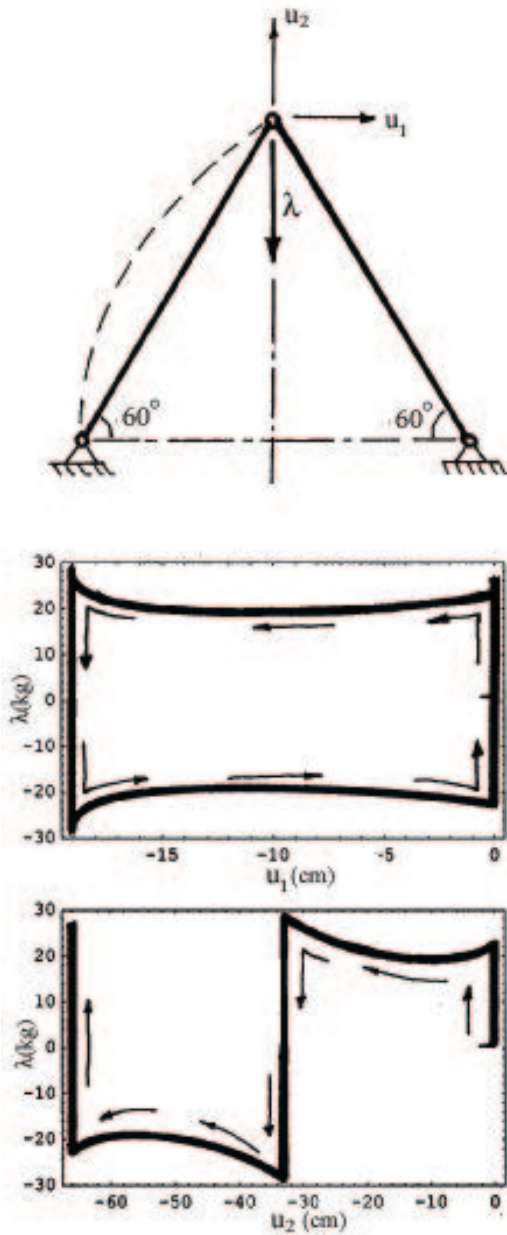


Figure 6 : Two-member truss. Equilibrium path: case 1.

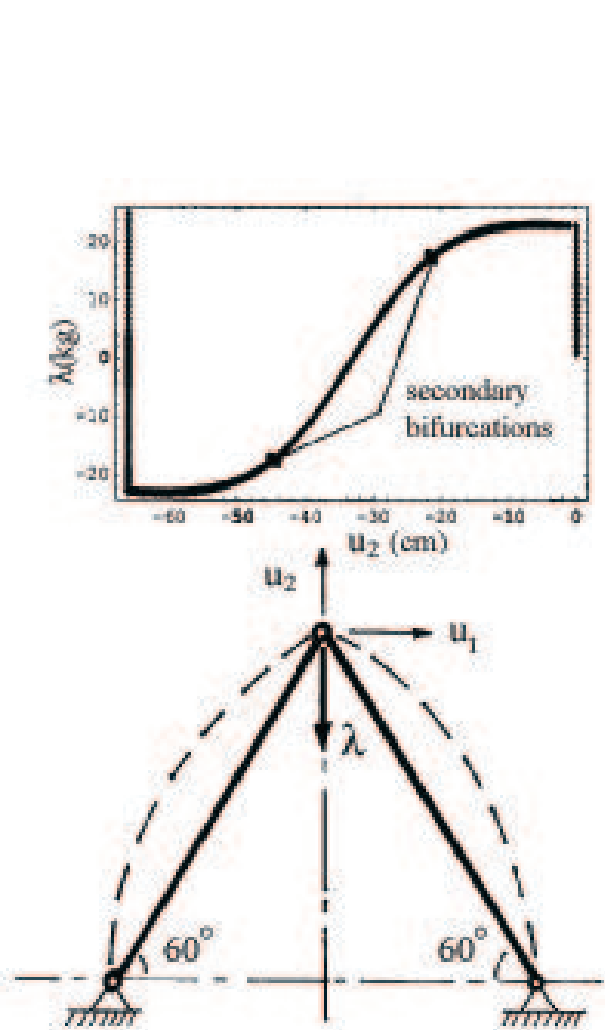


Figure 7 : Two-member truss. Equilibrium path: case 2.

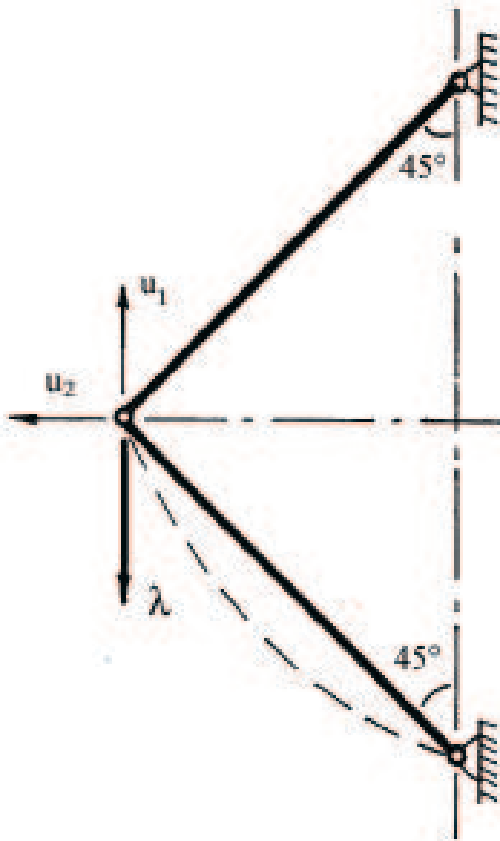


Figure 8 : Two-member truss. Equilibrium path: case 3.

cally. In the first loading case (Fig.6) the whole structure is unstable immediately after buckling of the left strut. However, the overall state becomes stable after passing the (local) limit point on the equilibrium path. Thus the truss with one buckled member is stable and can bear the increasing load. The stability is lost when the right strut becomes horizontal and the left strut is bent into a ring. The whole loading diagram looks like the complicated snap-through diagram. In the second loading case (Fig.7) the structure is unstable during the whole snap-through with two buckled members. This instability also includes the initial postbuckling range where the absolute magnitude of the vertical displacement increases with the increase of the load till the first (local) limit point. Two secondary branches emanating from the points shown in Fig.7 correspond to nonzero horizontal displacements of the node, that is the symmetry of the loaded configuration of the truss breaks. These secondary branches are unstable as well. In the third loading case (Fig.8) the whole equilibrium path is stable.

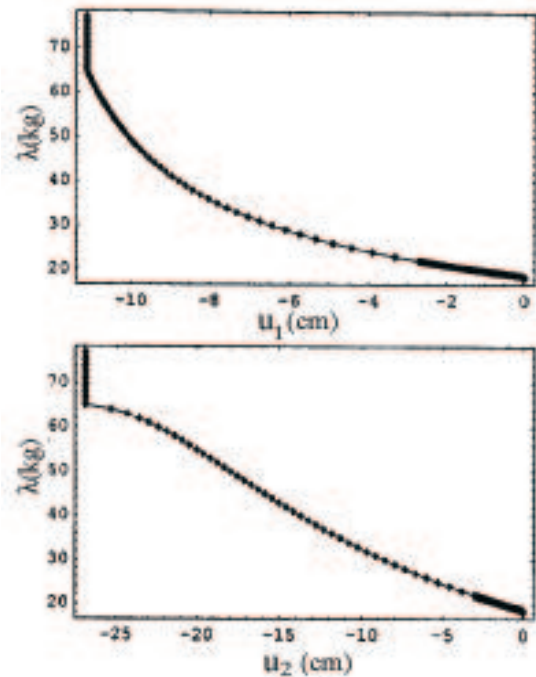


Figure 8 : Two-member truss. Equilibrium path: case 3.

4.3 Cable net

The pre-stressed cable net is loaded vertically as shown in Fig.9. This net comprises 29 members of the cross-section area $A = 0.01^2 \pi \text{ cm}^2$ and elasticity modulus $E = 10^6 \text{ kg/cm}^2$. Pre-stressing forces are given in Fig.10. The net deforms symmetrically. Members 2 and 29 ‘switch off’ at load $\lambda = 1.02 \text{ kg}$. Adjacent members 5 and 26 ‘switch off’ at load $\lambda = 4.47 \text{ kg}$. The deformed configuration together with the member forces is shown in Fig.10 at load $\lambda = 20 \text{ kg}$. It is important to underline that all deformation process is stable despite of ‘switching off’ of the adjacent cables. This fact corresponds to qualitative results of Volokh and Vilnay (2000).

4.4 Tensegrity ring

The pre-stressed tensegrity ring shown in Fig.11 may be used for modeling cytoskeletal structures of living cells. This ring comprises six nonintersecting struts (members 1-6) and twelve cables (members 7-18). The member properties are extracted from biological data (see Volokh et. al, 2000, for references): $E_c = 2.6 \text{ GPa}$, $A_c = 18 \text{ nm}^2$, $E_s = 1.2 \text{ GPa}$, $A_s = 190 \text{ nm}^2$, $(EI)_s = 2.15 \cdot 10^{-23} \text{ Nm}^2$. Subscript ‘s’ means strut and ‘c’ means cable. The length of struts is $\bar{L}_s = 3 \mu\text{m}$ at rest and corresponding buck-

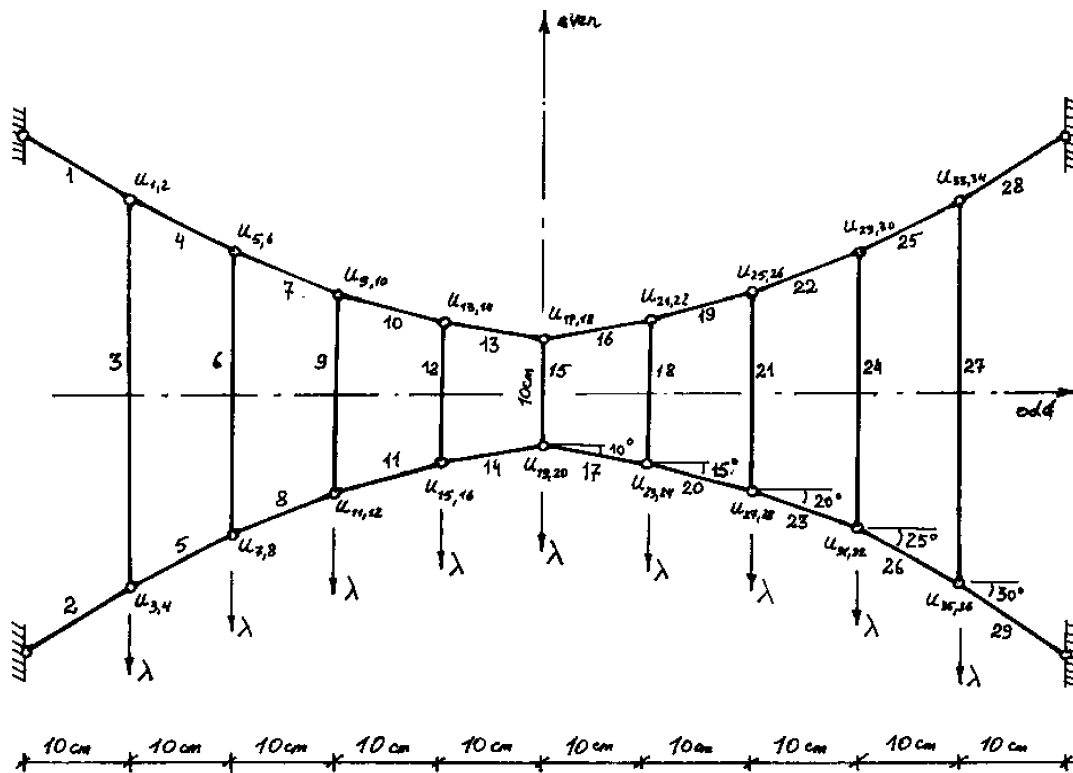


Figure 9 : Plane cable net.

ling force is $p_{cr} = 23.578 pN$. Cables are initially prestressed to $p_c = 3pN$. Consequently, the initial axial force in struts is $p_s = -2p_c \cos 75^\circ$. The initial elongation and the reference length for struts are $\Delta_s = p_s \bar{L}_s / (E_s A_s)$ and $L_s = \bar{L}_s + \Delta_s$ correspondingly. The reference length, the initial elongation, and the length at rest for cables are $L_c = 0.5L_s \sqrt{2 - \sqrt{3}}$, $\Delta_c = p_c \cdot L_c / (E_c A_c + p_c)$, $\bar{L}_c = L_c - \Delta_c$ correspondingly. The ring is 'twisted' by two loads λ applied perpendicular to strut 1 as shown in Fig.11.

The equilibrium path of this structure is traced up to load $\lambda = 45 pN$. The displacement of the node of intersection of members 1,12,13 in the direction of the applied force is given in Fig.12. The brief loading history is the following one. The pre-stressed ring is stable when $\lambda = 0 pN$. Cable 18 'switches off' when $\lambda = 3.5 pN$. Stability holds. Struts 2,3,4,5 buckle at $\lambda = 43.957 pN$. The load decreases and the equilibrium path is unstable up to $\lambda = 43.8657 pN$ where stability returns and the load increases. Strut 6 buckles at $\lambda = 44.4207 pN$ and the equilibrium path decreases unstably up to the point $\lambda = 44.0185 pN$. Passing this point the equilibrium path

increases up to $\lambda = 45 pN$ in a stable way.

5 Closure

A novel formulation for the analysis of pin-jointed assemblies with buckling and unilateral members has been proposed. The postbuckling behavior of slender struts is described by the highly accurate polynomial approximation of the solution of 'elastica' problem. Constitutive relations for structural members comprise two segments: before buckling and after buckling for strut-like members; and tension and compression for cable-like members. These constitutive relations are incorporated into the general path following procedures. The computational strategy of equilibrium analysis is discussed and the role of implicit branch switching is underlined. Numerical examples demonstrated efficiency and reliability of considered computational schemes.

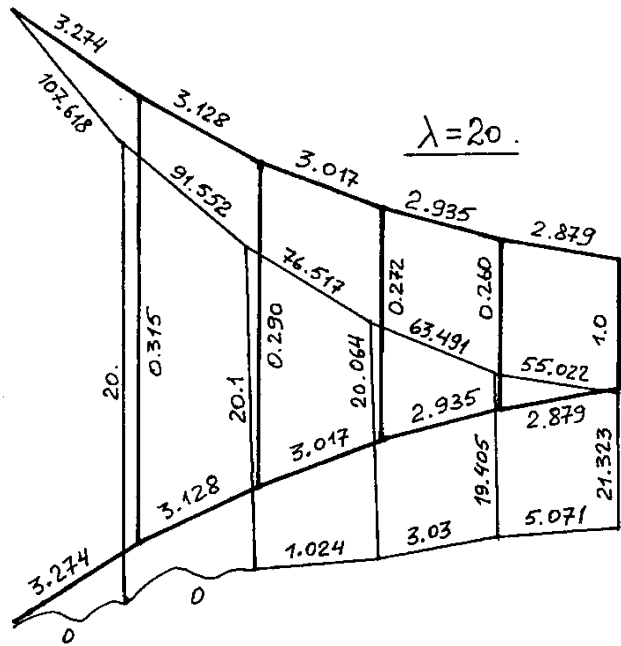


Figure 10 : Deformed configuration of the plane cable net at $\lambda = 20\text{kg}$.

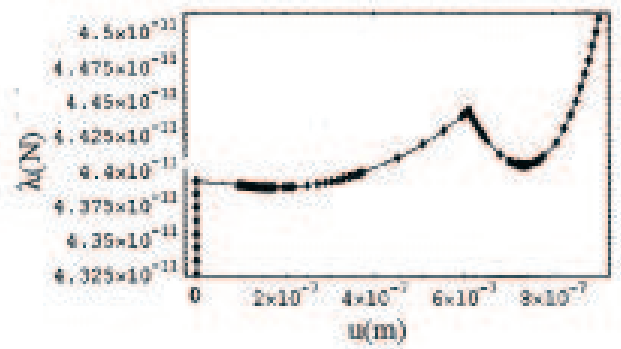


Figure 11 : External force versus displacement in its direction at the node of intersection of members 1,12,13 of the tensegrity ring.

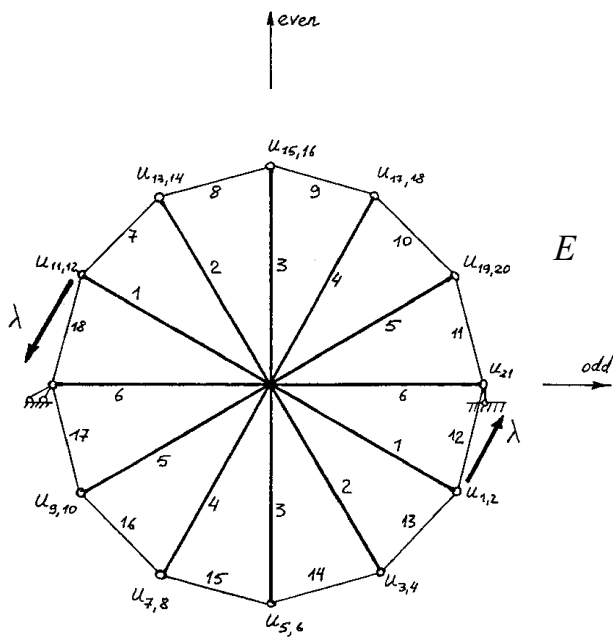


Figure 11 : Tensegrity ring.

References:

- Britvec, S.J.** (1973): *The stability of elastic systems*. Pergamon, NY.
- Buchholdt, N.A.** (1985): *Introduction to cable roof structures*. Cambridge University Press.
- Coughlin, M.F.; Stamenovich, D.** (1997): A tensegrity structure with buckling compression elements: Application to cell mechanics. *J Appl Mech* 64: 480-486.
- Crisfield, M.A.** (1991,1997): *Nonlinear analysis of solids and structures*, Vols 1,2. Wiley, Chichester.
- Fujii, F.; Okazawa, S.** (1997): Pinpointing bifurcation points and branch switching. *J Eng Mech* 123: 179-189.
- Ingber, D.E.** (1993): Cellular tensegrity: defining new rules of biological design that govern the cytoskeleton. *J Cell Science* 104: 613-627.
- Ingber, D.E.** (1998): The architecture of life. *Scientific American*, Jan: 30-39.
- Keller, H.B.** (1992): *Numerical methods for two-point boundary-value problems*. Dover, NY.
- Kondoh, K; Atluri, S.N.** (1985): Influence of local buckling on global instability: simplified, large deformation, post-buckling analyses of plane trusses. *Comp Struct* 21: 613-627.
- Kouhia, R.; Mikkola, M.** (1989): Tracing the equilibrium path beyond simple critical points. *Int J Num Meth Eng* 28: 2923-2941.
- Krishna, P.** (1978): *Cable-suspended roofs*. McGraw-Hill, NY.
- Magnusson, A.; Svensson, I.** (1998): Numerical treatment of complete load-deflection curves. *Int J Num Meth Eng* 41: 955-971.
- Riks, E.** (1998): Buckling analysis of elastic structures: a computational approach. *Adv Appl Mech* 34: 1-76.
- Seydel, R.** (1994): *Practical bifurcation and stability analysis: from equilibrium to chaos*, 2nd edn. Springer, NY.
- Sophianopoulos, D. S.; Michaltsos, G. T.** (2001): The Effect of a Rotational Spring on the Global Stability Aspects of the Classical von Mises Model under Step Loading, CMES: Computer Modeling in Engineering & Sciences, Vol.2, No.1,pp.15-26
- Szabo, J.; Kollar,L.** (1984): *Structural design of cable-suspended roofs*. Ellis Horwood, Chichester.
- Tanaka, T.; Kondoh, K; Atluri, S.N.** (1985) Instability analysis of space trusses using exact tangent stiffness method. *Finite Elem Anal Design* 1: 291-311.
- Timoshenko,S.P.; Gere,J.M.** (1961): *Theory of elastic stability*. McGraw-Hill, NY, 2nd edn.
- Volokh, K.Yu.** (1999): Nonlinear analysis of underconstrained structures. *Int J Solids Struct* 36: 2175-2187.
- Volokh, K.Yu.; Vilnay, O.** (2000): Why pre-tensioning stiffens cable systems. *Int J Solids Struct* 37: 1809-1816.
- Volokh, K.Yu.; Vilnay, O.; Belsky, M.** (2000): Tensegrity architecture explains linear stiffening and predicts softening of living cells. *J Biomech* 33: 1543-1549.
- Wolfram, S.** (1999): *Mathematica: a system for doing mathematics by computer*. Addison-Wesley, NY, 4th edn.
- Wriggers, P.** (1995): Solution strategies for nonlinear equations and computation of singular points. In: Kounadis, A.N. and Kratzig, W.B.: *Nonlinear stability of structures: theory and computational techniques*. Springer, NY.